Forward Elastic Scattering at High Energy in an $SU(3)$ Regge-Pole Model*

V. BARGER AND M. OLSSON
Department of Physics, University of Wisconsin, Madison, Wisconsin
(Received 24 January 1966)

The total-cross-section data on $\pi^{\pm}p$, $K^{\pm}p$, $K^{\pm}n$, pp, $\bar{p}p$, pn, and $\bar{p}n$ for laboratory momenta in the range 5 to 20 BeV/c are analyzed in terms of a meson-exchange model. The dynamics of the theoretical model for the forward scattering amplitude are provided by the Regge-pole amplitudes of the contributing exchanges; the total cross sections are obtained by the optical theorem. The allowed neutral, zero-strangeness meson exchanges are classified as members of established $SU(3)$ nonet or singlet multiplets. Certain linear combinations of the total cross sections are used in the analysis in order to separate the contributions of different $SU(3)$ multiplets according to signature under charge conjugation C. The odd-C exchanges are associated with the members [$\rho^0(760)$, $\phi(1020)$, $\omega(783)$] of the vector-meson nonet. The unitary-singlet Pomeranchuk Regge pole (P) and the Regge exchanges corresponding to the [$A_2(1310)$, $s_0(1525)$, $f_0(1250)$] members of the tensor nonet comprise the even-C exchanges. The residues of the Regge poles are related by $SU(3)$ symmetry. The model is consistent with the experimental total cross sections. A statistical fit to the data yields information on f/d ratios, Regge-pole residues, and trajectory intercepts at zero-momentum transfer. These parameters are in turn used to predict the real parts of the forward elastic-scattering amplitudes.

I. INTRODUCTION

THE observed forward peaking of high-energy elastic-scattering processes $A+B\rightarrow A+B$ is suggestive of meson exchange in the t channel: $\bar{A}+A\rightarrow \bar{B}+B$ (Fig. 1). A natural framework for this dynamical picture is provided by the Regge hypothesis in the pole approximation.[1–5] Incorporation of unitary-symmetry predictions for the Regge-pole residues yields a tractable model for a phenomenological analysis of high-energy elastic-scattering amplitudes. A critical analysis of the model becomes possible by restricting the study to total cross sections which are linearly related by the optical theorem to the imaginary part of the forward elastic amplitudes. The simplification which results at the forward direction is due to the following factors: (*i*) only the helicity non-flip s-channel amplitudes contribute, (*ii*) no assumption is required regarding the unknown momentum-transfer dependence of the residues and trajectories of the Regge poles, (*iii*) no interference terms arise between amplitudes of different trajectories as contrasted with the complex situation for the elastic differential cross sections, (*iv*) invariance principles can be used to isolate the contributions of trajectories with different isotopic-spin and charge-conjugation signature, and (*v*) symmetry-breaking effects are less critical than for the differential cross sections (e.g., a symmetry breakdown of $\sim$15% in the amplitude leads to $\sim$30% deviation in the differential cross section).

The contributing Regge meson exchanges are usually expected to correspond to physically observed particles. The experimentally observed mesons and meson resonances appear to belong to octet, singlet, or nonet representations of SU(3). In particular the pseudoscalar mesons [$\pi(140)$, $K(495)$, $\eta(550)$, $X^0(960)$] are satisfactorily classified as an octet and singlet. The vector mesons [$\rho(760)$, $K^*(890)$, $\phi(1020)$, $\omega(783)$] and the tensor mesons [$A_2(1310)$, $K^*(1430)$, $s_0(1525)$, $f_0(1250)$] exhibit nonet structure.[6,7] The identification of these meson states with $SU(3)$ representations is based on mass formulas and decay rates. Although a few other enhancements have been identified such as [$A_1(1080)$, $B(1220)$, $K^*(1175)$], they may prove to be of kinematic origin. Further arguments for not including these mesons as exchanges is given in Sec. II on the basis of their spin-parity assignments. In addition to the trajectories associated with the neutral members of the established nonet multiplets, we take into account the existence of a vacuum trajectory with maximal strength

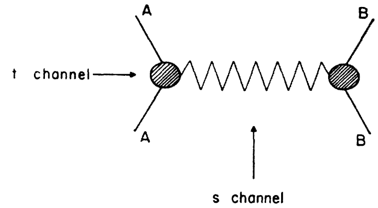

FIG. 1. Meson-exchange model for the elastic-scattering amplitude at high energy.

* Work supported in part by the U. S. Atomic Energy Commission under Contract No. AT(11-1)-881, COO-881-57.

[1] Some recent applications of the Regge-pole hypothesis to high-energy phenomena and sources of earlier literature can be found in Refs. 2–4 below.

[2] R. J. N. Phillips and W. Rarita, Phys. Rev. **140**, B200 (1965); **139**, B1336 (1965); **138**, B723 (1965); Phys. Rev. Letters **15**, 807 (1965); **14**, 502 (1965).

[3] T. Binford and B. Desai, Phys. Rev. **138**, B1167 (1965); B. Desai, *ibid.* **138**, B1174 (1965).

[4] B. M. Udgaonkar, in *Strong Interactions and High Energy Physics*, edited by R. G. Moorhouse (Plenum Press, Inc., New York, 1963), p. 223; Phys. Rev. Letters **8**, 142 (1962); A. Pignotti, Phys. Rev. **134**, B630 (1964); A. Ahmadzadeth, *ibid.* **134**, B633 (1964).

[5] R. K. Logan, Phys. Rev. Letters **14**, 414 (1965).

[6] S. Okubo, Phys. Letters **5**, 165 (1963).

[7] S. L. Glashow and R. H. Socolow, Phys. Rev. Letters **15**, 329 (1965); R. Delbourgo, M. A. Rashid, and J. Strathdee, *ibid.* **14**, 719 (1965).

(the Pomeranchuk trajectory) to be treated as a unitary singlet. This trajectory is required to explain the constancy of total cross sections at ultrahigh energy. (Cosmic-ray data[8] show no great change in total cross sections up to 10^4 BeV). Manifestations of this trajectory as an $I=0$, $J^{PG}=2^{++}$ meson is not absolutely essential since the trajectory may have a small slope at $t=0$. We take advantage of the $SU(3)$-representation classifications of the Regge poles to relate the intramultiplet residues. The trajectories within a particular multiplet are allowed to be nondegenerate in analogy with broken masses for the physical mesons.

In Sec. II an explicit statement of the model is given and individual Regge-pole amplitudes are isolated by the use of invariance principles. The contributions to the total cross sections of trajectories with odd (even) charge conjugation are analyzed in Sec. III (IV). Finally, in Sec. V the parameters of the fits are used to predict the real parts of the forward-scattering amplitudes.

II. STATEMENT OF MODEL

The phenomenological study of total cross sections at high energy is greatly faciliated by considering sums and differences of particle and antiparticle total cross sections:

$$\begin{aligned}\Delta_{AB}&\equiv\sigma_t(\bar{A}B)-\sigma_t(AB)\,,\\ \Sigma_{AB}&\equiv\sigma_t(\bar{A}B)+\sigma_t(AB)\,.\end{aligned}\tag{1}$$

With these combinations the exchanges of neutral, zero-strangeness mesons in the t channel are separated according to sign under charge conjugation C. Specifically, only exchanged mesons with odd C can contribute to the Δ_{AB}; only even-C exchanged mesons contribute to the Σ_{AB}. Further simplification results through invariance under isotopic-spin rotations by isolation of meson exchanges according to isotopic spin I. The neutral-meson exchange contributions of definite C and I are given in terms of the Δ's and Σ's by the following combinations:

$$\begin{aligned}&(C-,I=1)\begin{Bmatrix}\Delta_{\pi^+p}\\ \Delta_{K^+p}-\Delta_{K^+n}\\ \Delta_{pp}-\Delta_{pn}\end{Bmatrix};\quad (C+,I=1)\begin{Bmatrix}\Sigma_{K^+p}-\Sigma_{K^+n}\\ \\ \Sigma_{pp}-\Sigma_{pn}\end{Bmatrix};\\ &(C-,I=0)\begin{Bmatrix}\Delta_{K^+p}+\Delta_{K^+n}\\ \Delta_{pp}+\Delta_{pn}\end{Bmatrix};\quad (C+,I=0)\begin{Bmatrix}\Sigma_{\pi^+p}\\ \Sigma_{K^+p}+\Sigma_{K^+n}\\ \Sigma_{pp}+\Sigma_{pn}\end{Bmatrix}.\end{aligned}\tag{2}$$

For meson-nucleon scattering (Δ_{MN} and Σ_{MN}) the exchanged mesons must have natural parity $P=(-1)^J$ and charge conjugation $C=P$ because of the coupling to the external pseudoscalar meson pair. (The corresponding Regge pole must have signature $\tau=P$). For antinucleon-nucleon and nucleon-nucleon scattering it can again be shown that $\tau=P=C$ for the trajectories which make contributions to the spin averaged total cross sections.[9] Thus only mesons with $J^P=1^-$ and odd C can be exchanged in the Δ_{AB} and only mesons with $J^P=0^+$, 2^+ and even C can contribute to the Σ_{AB}. For the Δ_{AB} the vector mesons (ρ^0,ϕ,ω) are the only observed particles with the required quantum numbers. For the Σ_{AB} the members (A_2,s_0,f_0) of the tensor nonet can contribute. We include in addition the unitary singlet Pomeranchuk trajectory (P) with even C. Scalar exchanges (0^+, even C) should be negligible even if such particles are discovered because of their negative trajectory intercepts at $t=0$. On the basis of the above reasoning we conclude that the same meson exchanges, namely $[(\rho^0,\phi,\omega),\ (A_2,s_0,f_0),\ (P)]$, should account for all the quantities Σ_{MN}, Δ_{MN}, Σ_{NN}, Δ_{NN}. We explore this possibility in the following sections.

The dynamics of this model for the forward-scattering amplitude are described by Regge poles in the t channel as illustrated in Fig. 1. The asymptotic spin-averaged forward amplitude due to the Regge pole of a vector meson V may be written in natural units $\hbar=c=1$ as

$$f_{AB}{}^V(s,0)=\frac{\gamma_{AV}\gamma_{BV}}{4\pi s^{1/2}}\pi^{1/2}\frac{\Gamma(\alpha_V+\frac{3}{2})}{\Gamma(\alpha_V+1)}\frac{1-e^{-i\pi\alpha_V}}{\sin\pi\alpha_V}\times\left[\frac{s-M_A{}^2-M_B{}^2}{s_V}\right]^{\alpha_V}\tag{3}$$

where we have used the factorization theorem[10] for the dimensionless residue γ_{AVB}. Here s is the square of the total center-of-mass energy. α_V is the $t=0$ intercept of the vector-meson trajectory. s_V is an arbitrary scaling factor. The sign of the residue is assumed to be the sign at the physical vector-meson pole $t=m_V{}^2$.[11] The forward

[8] D. H. Perkins, in *Proceedings of the International Conference on Theoretical Aspects of Very High Energy Phenomena* (CERN, Geneva, 1961), p. 99.

[9] A. Ahmadzadeh and E. Leader, Phys. Rev. **134**, B1058 (1964); W. G. Wagner, Phys. Rev. Letters **10**, 202 (1963); D. H. Sharp and W. G. Wagner, Phys. Rev. **131**, 2226 (1963).

[10] M. Gell-Mann, Phys. Rev. Letters **8**, 263 (1962); V. N. Gribov and I. Ya. Pomeranchuk, *ibid.* **8**, 343, 412 (1962); J. M. Charap and E. J. Squires, Phys. Rev. **127**, 1387 (1962).

[11] Y. Hara, Progr. Theoret. Phys. (Kyoto) **28**, 1048 (1962); S. D. Drell, in *Proceedings of the 1962 Annual International Conference on High Energy Nuclear Physics at CERN*, edited by J. Prentki (CERN, Geneva, 1962), p. 897.

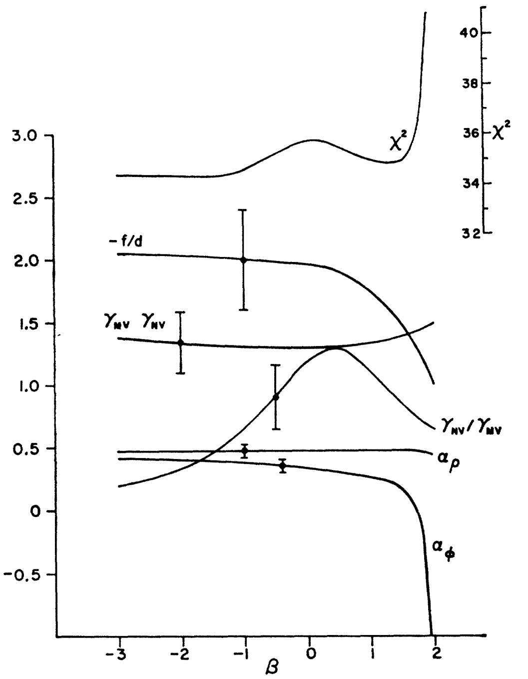

FIG. 2. Plot of the most likely solutions for the vector exchange parameters $\gamma_{MV}\gamma_{NV}$, γ_{MV}/γ_{NV}, $-f/d$, α_ρ,α_ϕ versus the parameter β [cf. Eqs. (13)–(17)]. Representative errors are given for each parameter. The values of χ^2 for the fits are indicated on the right ordinate.

amplitude due to a tensor Regge pole has the form

$$f_{AB}{}^T(s,0)=-\frac{\gamma_{AT}\gamma_{BT}}{4\pi s^{1/2}}\pi^{1/2}\alpha_T\frac{\Gamma(\alpha_T+\frac{3}{2})}{\Gamma(\alpha_T+1)}\times\frac{1+e^{-i\pi\alpha_T}}{\sin\pi\alpha_T}\left[\frac{s-M_A{}^2-M_B{}^2}{s_T}\right]^{\alpha_T}. \quad (4)$$

The factor α_T is extracted from the residue in order to avoid a ghost state at $\alpha_T=0$. The amplitude for the Pomeranchuk Regge pole is obtained from Eq. (4) by the replacement $T\to P$ and with $\alpha_P=1$. The resultant forward spin-averaged amplitude $f_{AB}(s,0)$ is given by a sum over the Regge amplitudes. By the optical theorem the total cross section is related to the imaginary part of the forward-scattering amplitude by

$$\sigma_t(AB)=[4\pi/q_{AB}(s)]\,\mathrm{Im}f_{AB}(s,0)\,, \quad (5)$$

where $q_{AB}(s)$ is the center-of-mass momentum. For later economy of notation we define

$$R_{AVB}(s)\equiv\frac{\pi^{1/2}}{s^{1/2}q_{AB}(s)}\frac{\Gamma(\alpha_V+\frac{3}{2})}{\Gamma(\alpha_V+1)}\left[\frac{s-M_A{}^2-M_B{}^2}{s_V}\right]^{\alpha_V},$$
$$R_{ATB}(s)\equiv\frac{\pi^{1/2}}{s^{1/2}q_{AB}(s)}\alpha_T\frac{\Gamma(\alpha_T+\frac{3}{2})}{\Gamma(\alpha_T+1)}\left[\frac{s-M_A{}^2-M_B{}^2}{s_T}\right]^{\alpha_T}. \quad (6)$$

In this model the scaling factors s_V, s_T, s_P are to be associated with the range of the t-channel exchange rather than with the masses of the external mesons.[3] This association is required to reproduce the $SU(3)$ sum rule for the Δ_{MB}.[12] We take a common value for the scaling factors associated with the exchanges of the members of the $SU(3)$ multiplet, e.g., $s_\rho=s_\omega=s_\phi\equiv s_V$. The actual numerical values of the multiplet scaling factors s_V, s_T, s_P are relevant only for a comparison of the residues at $t=0$ with the coupling constants at the physical poles. Such an extrapolation involves a knowledge of the t dependence of the residues which is beyond the scope of our phenomenological analysis. Consequently, we adopt the common value $s_V=s_T=s_P=(1\text{ BeV})^2$ for our analysis.

III. TOTAL-CROSS-SECTION DIFFERENCES (Δ_{AB})

According to the arguments of Secs. I and II, Regge exchanges associated with the (ρ^0,ϕ,ω) vector mesons should provide a quantitative explanation of the total-cross-section differences Δ_{MN} and Δ_{NN}. $SU(3)$ symmetry will now be utilized to relate the residues associated with the vector meson exchanges, thereby reducing the number of free parameters in the statistical fit.

The vector mesons $[\rho,K^*,\phi,\omega]$ are satisfactorily classified as an $SU(3)$ nonet which we designate by the 3×3 matrix V. The physical particles (ϕ,ω) are related to the octet and singlet representation members (ϕ_8,ω_1) by

$$\phi=(\sqrt{2}\phi_8-\omega_1)/\sqrt{3}\,,$$
$$\omega=(\phi_8+\sqrt{2}\omega_1)/\sqrt{3}\,. \quad (7)$$

This identification forbids the $\phi\to\rho+\pi$ decay mode. The relevant diagonal elements of V are given by

$$V_1{}^1=(\rho^0+\omega)/\sqrt{2}\,,$$
$$V_2{}^2=(-\rho^0+\omega)/\sqrt{2}\,, \quad (8)$$
$$V_3{}^3=-\phi\,.$$

The usual 3×3 matrices for the pseudoscalar-meson octet and the baryon octet[13] will be denoted by M and B, respectively. Then the general $SU(3)$-invariant interaction Lagrangian for the residues at $t=0$ of the vector-meson Regge poles has the form:

$$L_{VMM}=\sqrt{2}\gamma_{MV}\langle M[V,M]\rangle\,, \quad (9)$$
$$L_{V\bar{B}B}=\sqrt{2}\gamma_{NV}(f\langle\bar{B}[V,B]\rangle+d\langle\bar{B}\{V,B\}\rangle+\beta\langle V\rangle\langle\bar{B}B\rangle)\,, \quad (10)$$

where $\langle\ \ \rangle$ denotes trace over $SU(3)$ indices. We adopt the conventional normalization $f+d=1$. The residues of the vector-meson Regge poles can be expressed in terms of the $SU(3)$ parameters of Eqs. (9) and (10):

$$\tfrac{1}{2}\gamma_{\pi\rho}=\gamma_{K\rho}=\gamma_{K\phi}/\sqrt{2}=\gamma_{K\omega}=\gamma_{MV}\,, \quad (11)$$

[12] V. Barger and M. Rubin, Phys. Rev. 140, B1365 (1965); V. Barger and M. Olsson, Phys. Rev. Letters 15, 930 (1965).
[13] B. Sakita and K. C. Wali, Phys. Rev. 139, B1355 (1965).

$$\begin{aligned}\gamma_{p\rho}&=(f+d)\gamma_{NV}\,,\\ \gamma_{p\phi}&=\sqrt{2}(f-d-\beta)\gamma_{NV}\,,\\ \gamma_{p\omega}&=(f+d+2\beta)\gamma_{NV}\,.\end{aligned}\tag{12}$$

Combining the results of Eqs. (3), (5), (11), and (12), we obtain for the Δ_{MN} and Δ_{NN}:

$$\tfrac{1}{2}\Delta_{\pi^+p}=2\gamma_{MV}\gamma_{NV}R_{\pi\rho p}(s)\,,\tag{13}$$

$$\tfrac{1}{4}[\Delta_{K^+p}-\Delta_{K^+n}]=\gamma_{MV}\gamma_{NV}R_{K\rho p}(s)\,,\tag{14}$$

$$\tfrac{1}{4}[\Delta_{pp}-\Delta_{pn}]=\gamma_{NV}{}^2R_{p\rho p}(s)\,,\tag{15}$$

$$\begin{aligned}\tfrac{1}{4}[\Delta_{K^+p}+\Delta_{K^+n}]=&\,2(2f-1-\beta)\gamma_{MV}\gamma_{NV}R_{K\phi p}(s)\\ &+(1+2\beta)\gamma_{MV}\gamma_{NV}R_{K\omega p}(s)\,,\end{aligned}\tag{16}$$

$$\begin{aligned}\tfrac{1}{4}[\Delta_{pp}+\Delta_{pn}]=&\,2(2f-1-\beta)^2\gamma_{NV}{}^2R_{p\phi p}(s)\\ &+(1+2\beta)^2\gamma_{NV}{}^2R_{p\omega p}(s)\,.\end{aligned}\tag{17}$$

An immediate prediction of Eqs. (13) and (14) is

$$\begin{aligned}[\Delta_{K^+p}-\Delta_{K^+n}]/\Delta_{\pi^+p}=&\,[q_{\pi p}(s)/q_{Kp}(s)]\\ &\times[(s-M_K{}^2-M_p{}^2)/(s-M_\pi{}^2-M_p{}^2)]^{\alpha_\rho}\\ &\equiv R_{K\rho p}(s)/R_{\pi\rho p}(s)\,,\end{aligned}\tag{18}$$

which is the Regge-pole form of the $SU(3)$ sum rule,[12]

$$\Delta_{K^+p}=\Delta_{K^+n}+\Delta_{\pi^+p}\,,\tag{19}$$

derived by Barger and Rubin in the exact-symmetry limit of degenerate masses, $m_\pi=m_K$. The comparison of Eq. (18) with experiment is discussed at the end of this section.

The trajectories associated with the vector-meson nonet might reasonably be expected to be approximately parallel. Furthermore, each of the $\alpha_V(t)$ must intersect the value $J=1$ at $t=m_V{}^2$. Since $m_\omega\simeq m_\rho$ and $m_\phi>m_\rho$, the implication for the $t=0$ intercepts is $\alpha_\omega\simeq\alpha_\rho$ and $\alpha_\phi<\alpha_\rho$. As a working hypothesis we take $\alpha_\omega=\alpha_\rho$ and allow α_ρ and α_ϕ as free parameters. Nevertheless, we find that our solutions are quite insensitive to the precise value of α_ω in the interval $\alpha_\phi\leq\alpha_\omega\leq\alpha_\rho$.

The $T_3{}^3$ mass splitting of the members of the vector meson multiplet may be represented as

$$m^2=a\langle VV\rangle+b\langle\lambda VV\rangle+c\langle V\rangle^2+d\langle V\rangle\langle\lambda V\rangle\,,\tag{20}$$

where the 3×3 matrix λ is $\lambda_{\alpha\beta}=\delta_{\alpha3}\delta_{\beta3}$. With the Okubo "ansatz"[6] that terms involving $\langle V\rangle$ do not appear (i.e., $c=d=0$), the resulting mass formulas are

$$\begin{aligned}m_\omega{}^2&=m_\rho{}^2\,,\\ m_\phi{}^2&=2m_{K^*}{}^2-m_\rho{}^2\,.\end{aligned}\tag{21}$$

If this type of ansatz can be extended to nonet couplings, then we might expect that $\beta=0$ in Eq. (10). Nevertheless, we make no such restriction on the value of β in our analysis.

From Eqs. (13)–(17) the Δ_{MN} and Δ_{NN} are determined in terms of six independent parameters: β, γ_{MV}, γ_{NV}, f/d, α_ρ, α_ϕ, $(\alpha_\omega=\alpha_\rho)$. In the statistical analysis of the experimental data we fix the value of β and

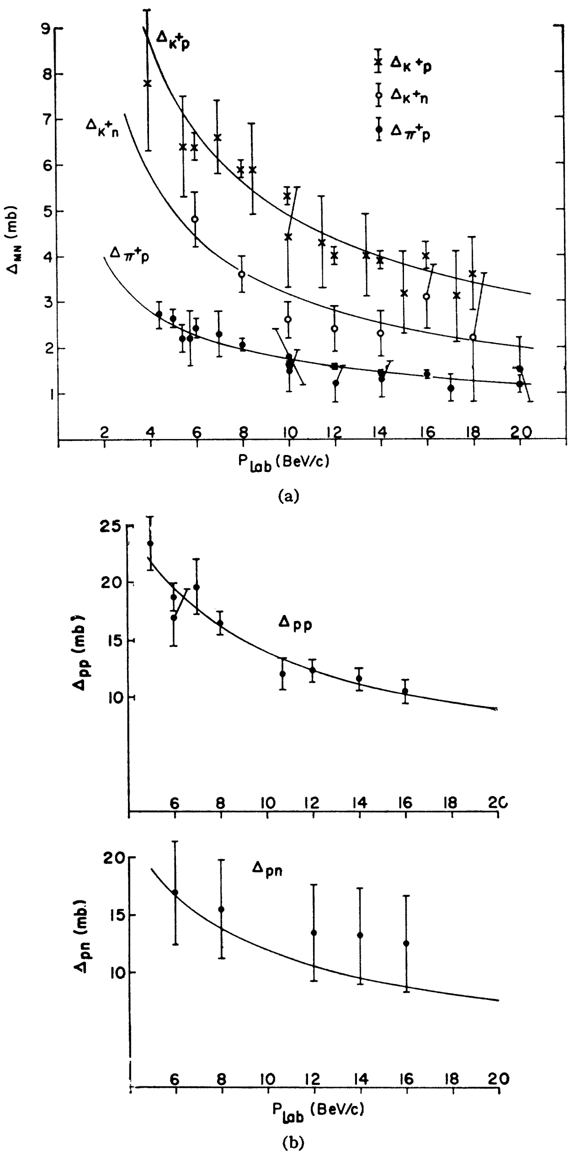

FIG. 3. Experimental measurements (Refs. 14–16) and theoretical curves for the total-cross-section differences: $\Delta_{AB}\equiv\sigma_t(\bar{A}B)-\sigma_t(AB)$. (a) Δ_{MN}; (b) Δ_{NN}. The theoretical curves were calculated using the parameters of Fig. 2 for $\beta=0$.

determine the remaining five parameters by minimizing χ^2. A total of 58 experimental measurements[14–16] in the

[14] W. Galbraith, E. W. Jenkins, T. F. Kycia, B. A. Leontic, R. H. Phillips, A. L. Read, and R. Rubinstein, Phys. Rev. (to be published); also R. H. Phillips (private communication).

[15] A. Citron *et al.*, Phys. Rev. Letters **13**, 205 (1964); W. F. Baker *et al.*, in *Proceedings of the Sienna International Conference on Elementary Particles and High-Energy Physics, 1963*, edited by G. Bernardini and G. P. Puppi (Società Italiana di Fisica, Bologna, 1963), Vol. I, p. 634; A. N. Diddens *et al.*, Phys. Rev. Letters **10**, 262 (1963); G. von Dardel *et al.*, *ibid.* **7**, 127 (1961); S. J. Lindenbaum *et al.*, *ibid.* **7**, 352 (1961); G. von Dardel *et al.*, *ibid.* **8**, 173 (1962).

[16] W. Galbraith *et al.*, Phys. Rev. **138**, B913 (1965); W. F. Baker *et al.*, *ibid.* **129**, 2285 (1963); S. J. Lindenbaum *et al.*, Phys. Rev. Letters **7**, 185 (1961); G. von Dardel, *ibid.* **5**, 333 (1960).

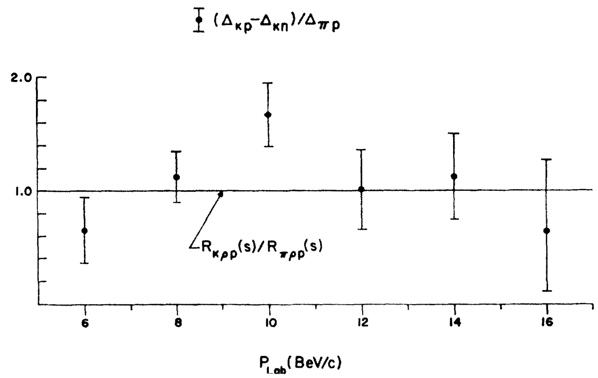

FIG. 4. Evaluation of the Regge pole form of the $SU(3)$ sum rule [cf. Eq. (18)]. The data points are the measured values (Ref. 14) for $(\Delta_{Kp}-\Delta_{Kn})/\Delta_{\pi p}$. The solid curve represents the kinematic factor $R_{K\rho p}(s)/R_{\pi\rho p}(s)$.

momentum interval 5 to 20 BeV/c were used in a statistical fit. The solutions for the parameters f/d, α_ρ, α_ϕ, $(\gamma_{NV}/\gamma_{MV})$, $(\gamma_{NV}\gamma_{MV})$ are plotted versus β in Fig. 2. For $\beta > 1.5$ the values of χ^2 were appreciably larger. For large negative values of β the ratio γ_{NV}/γ_{MV} becomes unreasonably small. For β in the interval $-3.0<\beta<1.5$, $\chi^2 \simeq 35$, which indicates an adequate fit of the model to the data. In Fig. 3 we show the fit with $\beta=0$.

The values of α_ρ and f/d are relatively insensitive to the value of β. For β in the interval $-3.0<\beta<1.0$ we find

$$\begin{aligned}\alpha_\rho &= 0.48\pm0.05\,,\\ f/d &= -2.0\pm0.7\,.\end{aligned} \tag{22}$$

The same values of f/d and α_ρ are also obtained from a fit to the Δ_{MN} alone. The f/d ratio as defined in Eq. (10) applies to the Regge pole residues at $t=0$. Since in general both the conventional γ_μ and $\sigma_{\mu\nu}$ vector-meson–nucleon couplings can contribute to the forward s-channel helicity nonflip Regge amplitude $f_{AB}{}^V(s,0)$,[9,17] the f/d ratio of Eq. (22) represents a combination of the electric- and magnetic-coupling contributions. Consequently the f/d ratio determined in Eq. (22) is not necessarily in disagreement with the widely accepted concept of pure f for the γ_μ coupling based on Sakurai's universality.[18]

The values of the fitted parameters can be used to evaluate the sum rule of Eq. (18). Both the experimental values[14] of the cross section ratio $[\Delta_{K^+p}-\Delta_{K^+n}]/\Delta_{\pi^+p}$ and the kinematic factor $[R_{K\rho p}(s)/R_{\pi\rho p}(s)]$ are plotted in Fig. 4. These should coincide if the Regge-pole form of the $SU(3)$ sum rule in Eq. (18) is satisfied. Quantitative agreement with experiment is indicated. In the Regge pole form of the $SU(3)$ sum rule the deviation from exact symmetry due to nondegenerate masses is contained in the kinematic factor. Since at high energies $[R_{K\rho p}(s)/R_{K\pi\rho p}(s)]$ is very nearly equal to the exact $SU(3)$ value of 1 (cf. Fig. 4), the external mass-splitting effect becomes unimportant. This accounts for the previous success of the unmodified $SU(3)$ sum rule.[12,19]

[17] L. Durand, III, and Y. Chiu (unpublished).

[18] J. J. Sakurai, in *Proceedings of the Enrico Fermi International School of Physics* (Academic Press Inc., New York, 1963), p. 41.

IV. TOTAL-CROSS-SECTION SUMS (Σ_{AB})

The analysis of the Σ_{AB} parallels the treatment in the previous section of the Δ_{AB}. According to the discussion in Secs. I and II, Regge exchanges associated with the tensor nonet (T) and a tensor unitary singlet (P) should account for the Σ_{MN} and Σ_{NN}. The symbols $[R,Q,S,P']$ are used to denote the Regge trajectories associated with the 2^+ nonet [$A_2(1310)$, $K^*(1430)$, $s_0(1525)$, $f_0(1250)$]. The diagonal elements of the 3×3 tensor nonet matrix T are given by

$$\begin{aligned}T_1{}^1 &= (R+P')/\sqrt{2}\,,\\ T_2{}^2 &= (-R+P')/\sqrt{2}\,,\\ T_3{}^3 &= -S\,.\end{aligned} \tag{23}$$

The general $SU(3)$-invariant Lagrangian for the residues at $t=0$ of the tensor-nonet Regge poles has the form:

$$L_{TMM}=\sqrt{2}\gamma_{MT}(\langle \mathrm{M}\{T,M\}\rangle+\epsilon\langle T\rangle\langle \mathrm{MM}\rangle)\,, \tag{24}$$
$$L_{T\bar{B}B}=\sqrt{2}\gamma_{NT}(F\langle\bar{B}[T,B]\rangle+D\langle\bar{B}\{T,B\}\rangle+\delta\langle T\rangle\langle\bar{B}B\rangle)\,,$$

where $F+D=1$. In terms of the $SU(3)$ parameters, the residues of the R, P', S Regge poles are given by

$$\begin{aligned}\gamma_{KR} &= \gamma_{MT}\,,\\ \tfrac{1}{2}\gamma_{\pi P'} &= -\gamma_{KS}/\sqrt{2}=(1+\epsilon)\gamma_{MT}\,,\\ \gamma_{KP'} &= (1+2\epsilon)\gamma_{MT}\,,\end{aligned} \tag{25}$$

and

$$\begin{aligned}\gamma_{pR} &= (F+D)\gamma_{NT}\,,\\ \gamma_{pP'} &= (F+D+2\delta)\gamma_{NT}\,,\\ \gamma_{pS} &= \sqrt{2}(F-D-\delta)\gamma_{NT}\,.\end{aligned} \tag{26}$$

The contribution of the Pomeranchuk Regge pole to the total cross sections is empirically well known to to much larger than the contributions of the secondary trajectories. Consequently in separating the Pomeranchuk and tensor-exchange contributions to the Σ_{AB}, the deviations from exact symmetry in the Pomeranchuk residues may become relatively important. For this reason we treat the Pomeranchuk residues $(\sqrt{2}\Gamma_{\pi P})$ and $(\sqrt{2}\Gamma_{KP})$ as independent parameters in our analysis. Exact symmetry residues would give $\Gamma_{\pi P}=\Gamma_{KP}$. The Pomeranchuk-nucleon residue is correspondingly defined as $(\sqrt{2}\Gamma_{NP})$.

[19] *Note added in proof.* An additional acceptable solution for the vector nonet parameters has been found with $\beta\approx 2f-1\approx 3$. In this solution ϕ is uncoupled from $\bar{N}N$ and $\alpha_\omega<\alpha_\rho$. The quantitative aspects of the fits obtained with this solution are essentially the same as those discussed above.

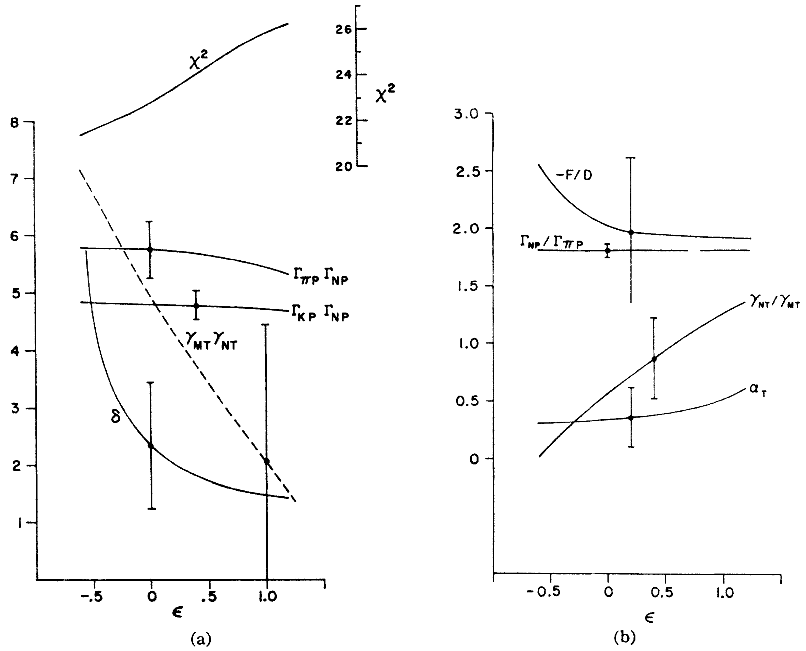

FIG. 5. Plot of the most likely solutions for the tensor exchange parameters: (a) $\Gamma_{KP}\Gamma_{NP}$, $\Gamma_{\pi P}\Gamma_{NP}$, $\gamma_{MT}\gamma_{NT}$, δ; (b) $\Gamma_{NP}/\Gamma_{\pi P}$, γ_{NT}/γ_{MT}, $-F/D$, α_T, versus the parameter ϵ [cf. Eqs. (27)–(31)]. Representative errors are given for each parameter. The values of χ^2 for the fits are indicated on the right ordinate of (a).

We now can write the Σ_{MN} and Σ_{NN} in terms of the P, R, P', S Regge amplitudes. From Eqs. (4), (5), (25), and (26), we obtain

$$\tfrac{1}{4}[\Sigma_{K^+p}-\Sigma_{K^+n}]=\gamma_{MT}\gamma_{NT}R_{KRp}(s)\,, \tag{27}$$

$$\tfrac{1}{4}[\Sigma_{pp}-\Sigma_{pn}]=\gamma_{NT}{}^2R_{pRp}(s)\,, \tag{28}$$

$$\tfrac{1}{2}\Sigma_{\pi^+p}=2\Gamma_{\pi P}\Gamma_{NP}R_{\pi Pp}(s)+2(1+\epsilon)(1+2\delta)\gamma_{MT}\gamma_{NT}R_{\pi P'p}(s)\,, \tag{29}$$

$$\begin{aligned}\tfrac{1}{4}[\Sigma_{K^+p}+\Sigma_{K^+n}]=&\,2\Gamma_{KP}\Gamma_{NP}R_{KPp}(s)\\&+(1+2\epsilon)(1+2\delta)\gamma_{MT}\gamma_{NT}R_{KP'p}(s)\\&-2(1+\epsilon)(2F-1-\delta)\gamma_{MT}\gamma_{NT}R_{KSp}(s)\,,\end{aligned} \tag{30}$$

$$\begin{aligned}\tfrac{1}{4}[\Sigma_{pp}+\Sigma_{pn}]=&\,2\Gamma_{NP}{}^2R_{pPp}(s)+(1+2\delta)^2\gamma_{NT}{}^2\\&\times R_{pP'p}(s)+2(2F-1-\delta)^2\gamma_{NT}{}^2R_{pSp}(s)\,.\end{aligned} \tag{31}$$

In analogy with the discussion in Sec. III the mass relations $m_{f_0}\simeq m_{A_2}$ and $m_{s_0}>m_{A_2}$ lead us to expect $\alpha_{P'}\simeq\alpha_R$ and $\alpha_S<\alpha_R$. Inasmuch as the data on the Σ_{AB} are less accurate than the data on the Δ_{AB}, the sensitivity to the tensor-nonet trajectory intercepts is reduced. For this reason we use degenerate trajectory intercepts $\alpha_{P'}=\alpha_R=\alpha_S\equiv\alpha_T$ for the analysis. However, our solutions are unaffected by variations of α_S in the interval $0\leq\alpha_S\leq\alpha_R$.

The decay rates of the tensor nonet mesons have been satisfactorily explained with no $\langle T\rangle\langle MM\rangle$ coupling term, $\epsilon=0$. Since ϵ is a parameter of the $SU(3)$ space it will not be momentum-transfer independent. Consequently we also expect that $\epsilon\simeq0$ at $t=0$. Although *a priori* we place no restriction on ϵ, we find for reasonable solutions that ϵ must be small.

For a fixed value of ϵ, Eqs. (27)–(31) contain eight independent parameters: $\Gamma_{\pi P}$, Γ_{KP}, Γ_{NP}, γ_{MT}, γ_{NT}, F/D, δ, α_T. We determine these eight parameters by minimizing χ^2 in a statistical fit to 35 measurements of the Σ_{AB} given by Galbraith *et al.*[16] The solutions for the parameters are plotted versus ϵ in Fig. 5. Solutions with reasonable values of the parameters could be found only for ϵ in the interval $-0.5<\epsilon<1.0$. The χ^2's for these solutions are less than 26 [Fig. 5(a)] indicating adequate fits to the data. For negative ϵ the $\langle T\rangle\langle\bar{B}B\rangle$ coupling strength becomes dominant and the ratio γ_{NT}/γ_{MT} goes linearly to zero as ϵ approaches -0.5. According to the analysis of the 2^+ meson decay rates, the most attractive solution is for $\epsilon=0$. In Fig. (6) we show the fit for $\epsilon=0$. For this particular choice of ϵ, we see from Fig. (5b) that the F/D ratio of Eq. (24) for the tensor nonet $\bar{B}B$ residues at $t=0$ is given by

$$F/D=-2.0\pm0.6\,. \tag{32}$$

This value for the F/D ratio of the $T\bar{B}B$ coupling is numerically coincident with the f/d ratio determination of Eq. (22) for the $V\bar{B}B$ residues. This rather striking numerical equality suggests that there may be a basic reason for a universal value. The nonet trajectory intercept for $\epsilon=0$ is

$$\alpha_T=0.39\pm0.24\,. \tag{33}$$

Deviation from the exact-symmetry coupling prediction $\Gamma_{\pi P}=\Gamma_{KP}$ for the unitary-singlet Pomeranchuk meson residues is apparent from the curves for $\Gamma_{\pi P}\Gamma_{NP}$ and $\Gamma_{KP}\Gamma_{NP}$ in Fig. 5(a). For $\epsilon=0$, we find

$$(\Gamma_{\pi P}/\Gamma_{KP})=1.19\pm0.05 \tag{34}$$

indicating a 20% deviation from exact symmetry. The quoted error on the ratio in Eq. (34) is smaller than

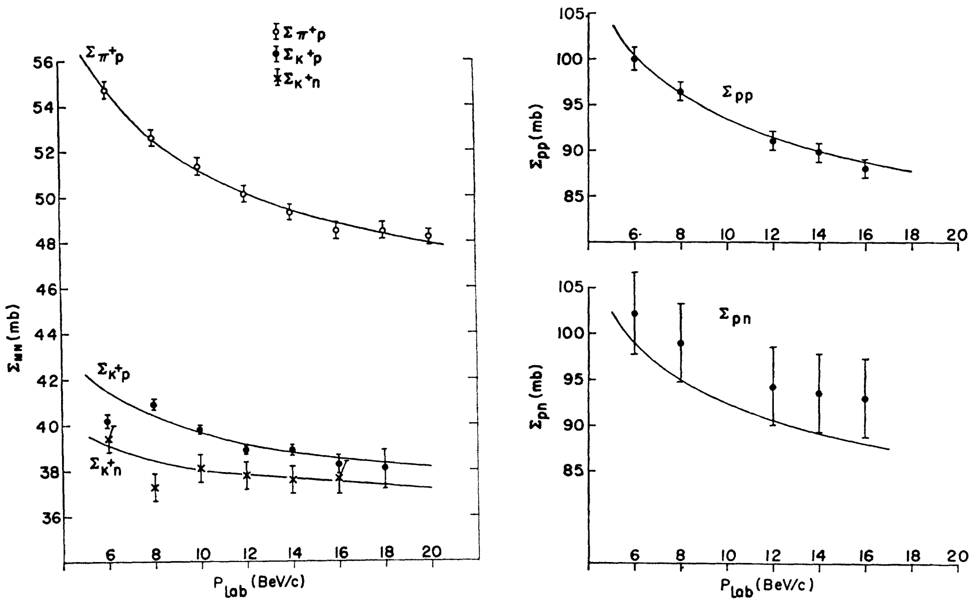

(a) (b)

FIG. 6. Experimental measurements (Refs. 14–16) and theoretical curves for total-cross-section sums: $\Sigma_{AB} \equiv \sigma_t(\bar{A}B) - \sigma_t(AB)$. (a) Σ_{MN}; (b) Σ_{NN}. The theoretical curves were calculated using the parameters of Fig. 5 for $\epsilon = 0$.

would be inferred from Fig. 5(a) due to the inclusion of the error correlation.

A final interesting feature of the Σ_{AB} analysis is the requirement of a relatively large positive value for the $\langle T\rangle\langle\bar{B}B\rangle$ coupling strength δ, as shown in Fig. 5(a). The effect of large δ (and $F\approx 2$) is to enhance the P' amplitude in Eqs. (29), (30), and (31) relative to the R and S amplitudes.

V. FORWARD ELASTIC AMPLITUDES

Separate analysis of the Σ_{AB} and the Δ_{AB} as in Secs. III and IV avoids unphysical correlations of the parameters of the odd-C exchanges with the parameters of the even-C exchanges. The statistical accuracy of this method is thereby improved over that of a direct analysis of the $\sigma_t(AB)$. We now make use of the parameters determined in Secs. III and IV to calculate the over-all fits to the total-cross-section data. We focus our attention on the solution $\beta = \epsilon = 0$. The quantitative features of the fits are the same for the other values of β and ϵ in Fig. 2 and Fig. 5. We summarize here the numerical values of the parameters:

Pomeranchuk parameters:

$$\Gamma_{\pi P} = 1.78 \pm 0.08\,,\quad \Gamma_{KP} = 1.50 \pm 0.06\,,\quad \Gamma_{NP} = 3.20 \pm 0.13\,. \tag{35}$$

Tensor-nonet parameters:

$$\gamma_{MT} = 2.7 \pm 1.5\,,\quad \gamma_{NT} = 1.7 \pm 1.5\,,\quad F/D = -2.0 \pm 0.6\,,\quad \alpha_T = 0.39 \pm 0.24\,,\quad \delta = 2.3 \pm 1.1\,. \tag{36}$$

TABLE I. Contributions to the total cross section from the individual Regge pole amplitudes at $P_{\rm Lab} = 12$ BeV/c.

$P_{\rm Lab} = 12$ BeV/c Reaction	$\sigma_t = \frac{4\pi}{q}\,{\rm Im}f(s,0)$ (mb)	Pomeranchuk singlet P	Tensor nonet R^0 (A_2)	Tensor nonet S (s_0)	Tensor nonet P' (f_0)	Vector nonet ρ^0	Vector nonet ϕ	Vector nonet ω
π^-p	25.9	20.9	0	0	4.2	0.8	0	0
π^+p	24.3	20.9	0	0	4.2	−0.8	0	0
K^-p	21.8	17.6	0.4	−0.5	2.1	0.4	1.4	0.4
K^+p	17.4	17.6	0.4	−0.5	2.1	−0.4	−1.4	−0.4
K^-n	20.2	17.6	−0.4	−0.5	2.1	−0.4	1.4	0.4
K^+n	17.4	17.6	−0.4	−0.5	2.1	0.4	−1.4	−0.4
$\bar{p}p$	51.9	37.8	0.2	0.2	7.5	0.5	5.2	0.5
pp	39.5	37.8	0.2	0.2	7.5	−0.5	−5.2	−0.5
$\bar{p}n$	50.4	37.8	−0.2	0.2	7.5	−0.5	5.2	0.5
pn	40.0	37.8	−0.2	0.2	7.5	0.5	−5.2	−0.5

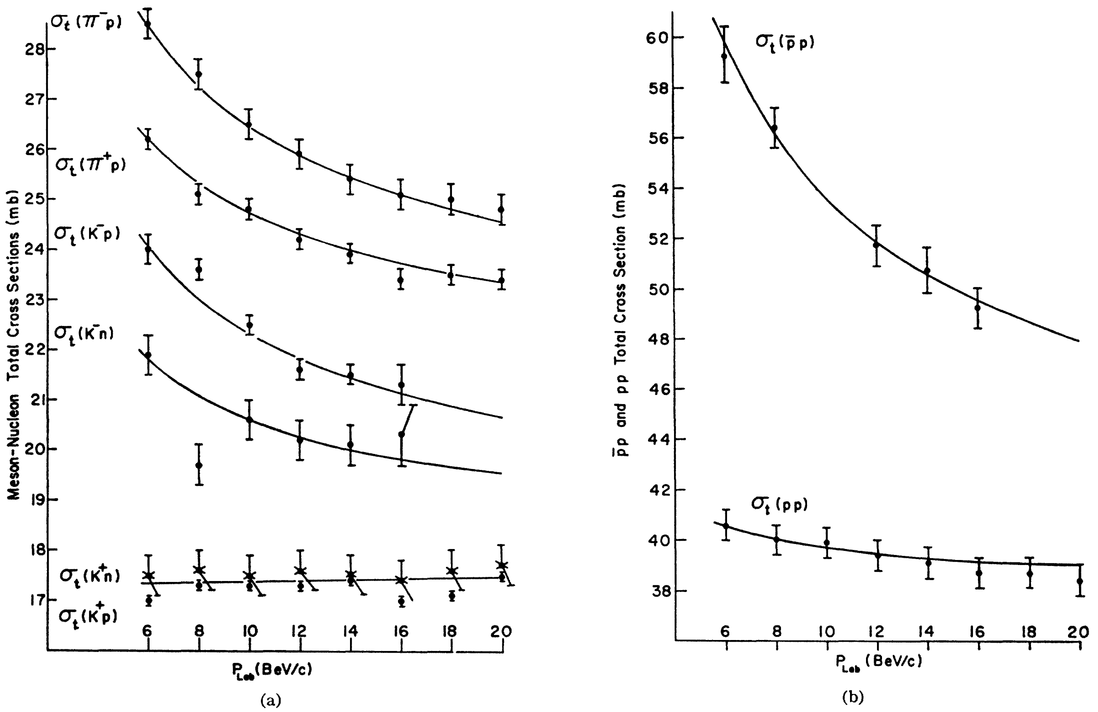

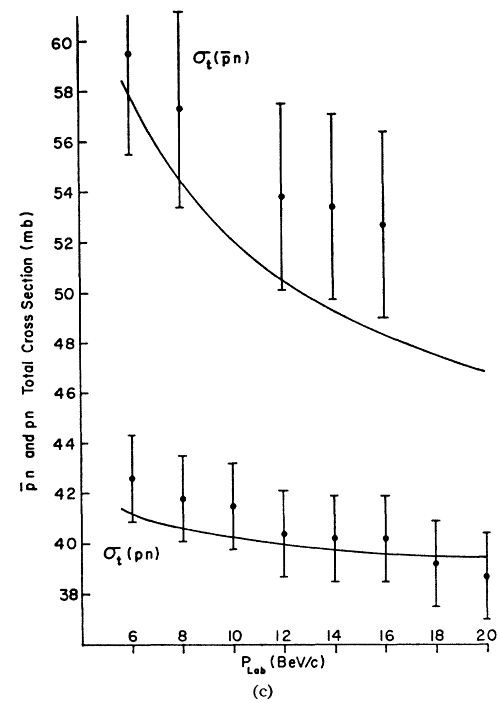

FIG. 7. Experimental measurements (Refs. 14–16) and theoretical curves for the total-cross sections from the results of Figs. 5 and 6. (a) $\sigma_t(\pi^\pm p)$, $\sigma_t(K^\pm p)$, $\sigma_t(K^\pm n)$; (b) $\sigma_t(\bar{p}p)$, $\sigma_t(pp)$; (c) $\sigma_t(\bar{p}n)$, $\sigma_t(pn)$. The theoretical curves for $\sigma_t(K^+n)$ and $\sigma_t(K^+p)$ in (a) are not resolved on this scale.

Vector-nonet parameters:

$$\begin{aligned} \gamma_{MV} &= 1.03 \pm 0.08, \\ \gamma_{NV} &= 1.25 \pm 0.26, \\ f/d &= -2.0 \pm 0.4, \\ \alpha_\rho = \alpha_\omega &= 0.48 \pm 0.05, \\ \alpha_\phi &= 0.33 \pm 0.06. \end{aligned} \tag{37}$$

The resultant fit to the total-cross-section data is shown in Figs. 7(a), 7(b), and 7(c). The over-all $\chi^2 \simeq 58$ with 80 degrees of freedom. The theoretical curves in Figs. 7(a) and 7(b) are in good agreement with the data. In Fig. 7(c) the calculated curve for $\sigma_t(\bar{p}n)$ tends to fall about one standard deviation below the data points. We can trace the cause of this discrepancy to Δ_{pn} and Σ_{pn} in Figs. 3(b) and 6(b). Since the relative shift

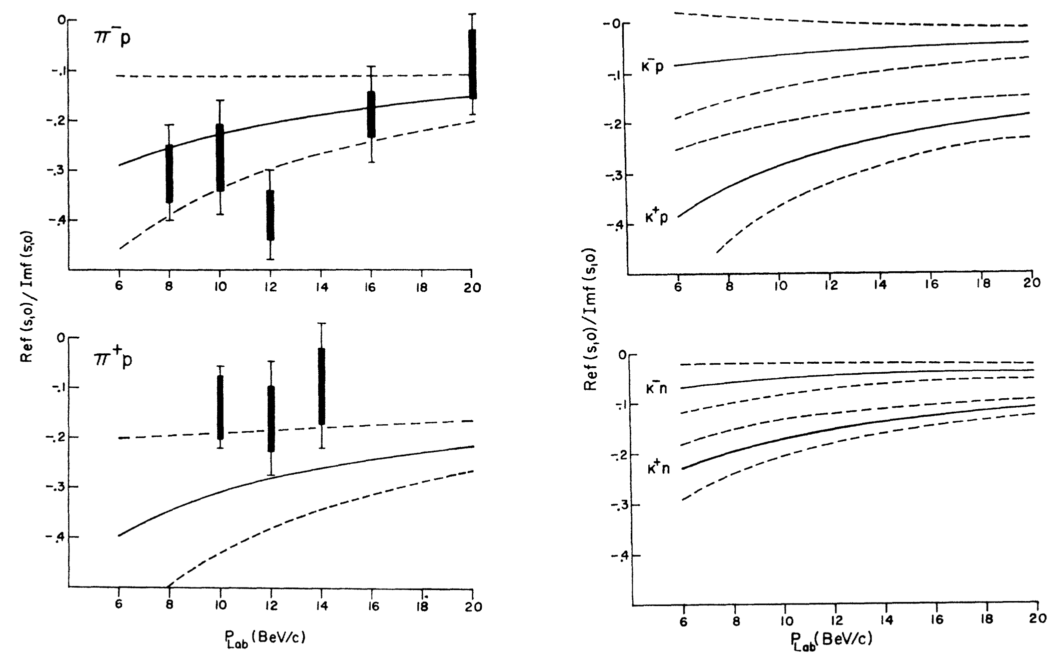

(a)

(b)

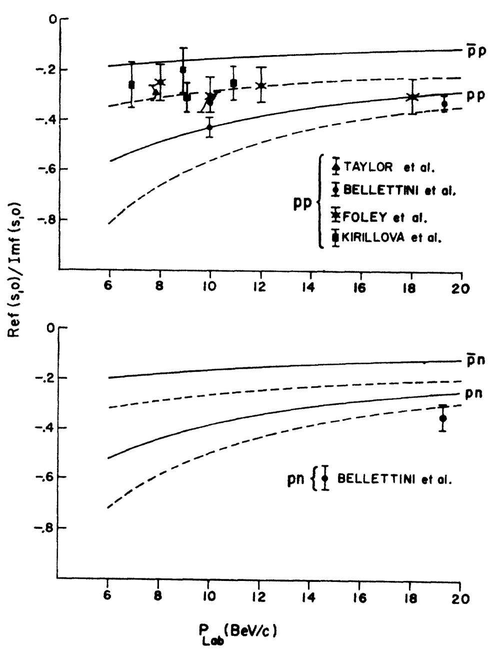

(c)

FIG. 8. Experimental data and theoretical prediction for the ratio of real to imaginary parts of the forward-scattering amplitudes: (a) $\pi^{\pm}p$ (Ref. 20); (b) $K^{\pm}p$, $K^{\pm}n$; (c) $\bar{p}p$, pp (Ref. 21), $\bar{p}n$, pn (Ref. 22). The dashed curves representing error corridors of the statistical analysis of the total-cross-section data are shown for all but $\bar{p}p$ and $\bar{p}n$. The error on the data point for Ref/Imf of pn scattering (Ref. 22) in (c) includes only experimental statistical error.

between theory and experiment occurs for both Δ_{pn} and Σ_{pn}, the discrepancy could not be described in terms of the exchange of one additional $SU(3)$ multiplet. In terms of our model, Eqs. (15) and (28) require that $\Delta_{pp}>\Delta_{pn}$ and $\Sigma_{pp}>\Sigma_{pn}$. Adding these inequalities we obtain the requirement that $\sigma_t(\bar{p}p)>\sigma_t(\bar{p}n)$. Although the present measurements of $\sigma_t(\bar{p}n)$ have quite large error bars,[16] they do suggest that $\sigma_t(\bar{p}n)$ systematically exceeds $\sigma_t(\bar{p}p)$. Hence a definite test of our model would be an accurate experimental determination of $[\sigma_t(\bar{p}p)-\sigma_t(\bar{p}n)]$.

In Table I the contributions to the total cross sections of each Regge pole amplitude are tabulated for laboratory momentum 12 BeV/c (for $\epsilon=\beta=0$). The importance of deviations from exact symmetry for the Pomeranchuk contribution to π and K scattering is apparent from Table I. The dominance of the P' amplitude among the tensor nonet Regge poles is due

TABLE II. Contributions to the real part of the forward-scattering amplitude from the individual Regge-pole amplitudes at $P_{\mathrm{Lab}}=12$ BeV/c.

$P_{\mathrm{Lab}}=12$ BeV/c Reaction	$\frac{4\pi}{q}\mathrm{Re}f(s,0)$ (mb)	Pomeranchuk singlet P	Tensor nonet R^0 (A_2)	Tensor nonet S (s_0)	Tensor nonet P' (f_0)	Vector nonet ρ^0	Vector nonet ϕ	Vector nonet ω
π^-p	-5.4	0	0	0	-6.1	0.7	0	0
π^+p	-6.8	0	0	0	-6.1	-0.7	0	0
K^-p	-1.3	0	-0.5	0.7	-3.1	0.4	0.8	0.4
K^+p	-4.5	0	-0.5	0.7	-3.1	-0.4	-0.8	-0.4
K^-n	-1.1	0	0.5	0.7	-3.1	-0.4	0.8	0.4
K^+n	-2.6	0	0.5	0.7	-3.1	0.4	-0.8	-0.4
$\bar{p}p$	-7.4	0	-0.3	-0.3	-10.8	0.5	3.0	0.5
pp	-15.4	0	-0.3	-0.3	-10.8	-0.5	-3.0	-0.5
$\bar{p}p$	-7.8	0	0.3	-0.3	-10.8	-0.5	3.0	0.5
pn	-13.8	0	0.3	-0.3	-10.8	0.5	-3.0	-0.5

to the relatively large $\langle T\rangle\langle\bar{B}B\rangle$ coupling strength δ and $F/D\approx -2$. The ϕ is the dominant vector nonet amplitude[19] due to $f/d\approx -2$. The empirical regularity of high-energy KN total cross sections, namely, $\sigma_t(K^+p)\approx\sigma_t(K^+n)\approx$ constant, can be expressed in terms of the Regge-pole amplitudes. Since only the R and ρ amplitudes differ in sign between $\sigma_t(K^+p)$ and $\sigma_t(K^+n)$ we have

$$\sigma_t(K^+p)-\sigma_t(K^+n)=\frac{8\pi}{q}[\mathrm{Im}f^R(s,0)-\mathrm{Im}f^\rho(s,0)]. \tag{38}$$

Thus the equality $\sigma_t(K^+p)\approx\sigma_t(K^+n)$ implies $\mathrm{Im}f^R(s,0)\approx\mathrm{Im}f^\rho(s,0)$.[2,4] This is indeed the case in Table I. The constancy of $\sigma_t(K^+p)$ or $\sigma_t(K^+n)$ requires that the total contribution of the tensor nonet cancel the total contribution of the vector nonet.

For $\bar{N}N$ and NN total cross sections, we observe from Table I that the P' and ϕ amplitudes[19] are principally responsible for the variations with energy. These two amplitudes add constructively for $\sigma_t(\bar{N}N)$ and destructively for $\sigma_t(NN)$.

The real part of the forward Regge pole amplitude is given by Eqs. (3) and (4) as

$$\mathrm{Re}f_{AB}{}^V(s,0)=\tan(\pi\alpha_V/2)\mathrm{Im}f_{AB}{}^V(s,0) \tag{39}$$

for a vector-meson exchange, and

$$\mathrm{Re}f_{AB}{}^T(s,0)=-\cot(\pi\alpha_T/2)\mathrm{Im}f_{AB}{}^T(s,0) \tag{40}$$

for a tensor-meson exchange. Consequently the Regge-pole parameters determined from the total-cross-section analysis may now be used to predict the real parts of the forward-scattering amplitudes. A particularly straightforward result which follows from Eqs. (13) and (39) is the prediction

$$\mathrm{Re}f_{\pi^-p}(s,0)>\mathrm{Re}f_{\pi^+p}(s,0)\,. \tag{41}$$

Furthermore, since $\sigma_t(\pi^-p)>\sigma_t(\pi^+p)$ (Ref. 14), and $\mathrm{Re}f_{\pi^\pm p}<0$,[20] the qualitative restriction of the model given in Eq. (41) may be expressed as

$$\rho_{\pi^-p}>\rho_{\pi^+p}\,, \tag{42}$$

where

$$\rho_{AB}\equiv\mathrm{Re}f_{AB}(s,0)/\mathrm{Im}f_{AB}(s,0)\,. \tag{43}$$

In Figs. 8(a), 8(b), and 8(c) we compare the experimental data[20–22] on the ρ_{AB} with the theoretical predictions based on the statistical analysis (with $\beta=\epsilon=0$) of the total cross sections. The solid and dashed curves represent the predicted mean values and error corridors, respectively, for the ρ_{AB}. The prediction for ρ_{π^-p} in Fig. 8(a) fits the data[20] quite well. Although the data on ρ_{π^+p} are consistent with the predicted values, the data points are systematically higher than the theoretical curve. In fact the data appear to violate the condition in Eq. (42). Precise experimental determination of $[\rho_{\pi^-p}-\rho_{\pi^+p}]$ will provide another significant test of the model. The ρ_{KN}, $\rho_{\bar{K}N}$, ρ_{NN}, and $\rho_{\bar{N}N}$ are shown in Figs. 8(b) and 8(c). ρ_{K^-p}, ρ_{K^-n}, $\rho_{\bar{p}p}$, and $\rho_{\bar{p}n}$ are predicted to be small whereas ρ_{K^+p}, ρ_{K^+n}, ρ_{pp}, and ρ_{pn} are appreciably in size. A number of experimental determinations[21] exist for ρ_{pp} as indicated in Fig. 8(c). More recently ρ_{pn} has been deduced at 19.3 BeV/c from the pd elastic differential cross section.[22] A consistent fit to the pd scattering data could be obtained only with the condition $\rho_{pn}\approx\rho_{pp}$. This result is in essential agreement with the prediction derived from the analysis of the total cross sections as shown in Fig. 8(c).

In Table II the contributions of the individual Regge pole amplitudes to the real parts of the forward-scattering amplitudes are tabulated for laboratory momentum 12 BeV/c. The dominance of the P' amplitude accounts mainly for the negative values of all the real parts. The destructive addition of the tensor and

[20] K. J. Foley *et al.*, Phys. Rev. Letters **14**, 862 (1965).

[21] K. J. Foley *et al.*, Phys. Rev. Letters **14**, 74 (1965); G. Bellettini *et al.*, Phys. Letters **14**, 164 (1965); **19**, 705 (1966); A. E. Taylor *et al.*, *ibid.* **14**, 54 (1965); L. F. Kirillova *et al.*, Soviet J. Nucl. Phys. **1**, 379 (1965).

[22] G. Bellettini *et al.*, Phys. Letters **19**, 341 (1965).

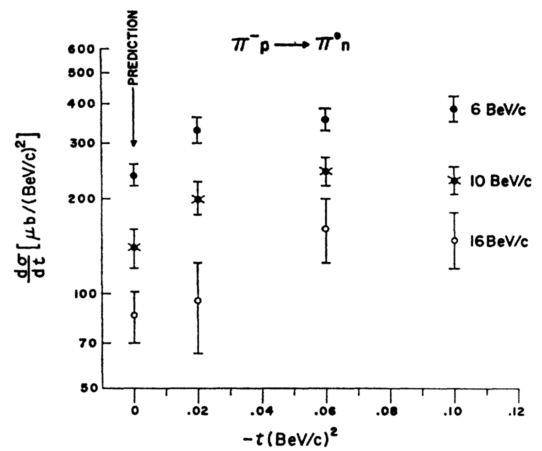

FIG. 9. Differential cross section for the charge-exchange reaction $\pi^- p \rightarrow \pi^0 n$. The $t=0$ value of $d\sigma/dt$ predicted from the analysis of the total cross sections is compared with measured values (Ref. 23) at nonzero momentum transfer.

vector contributions required for constant $\sigma_t(K^+p)$ and $\sigma_t(K^+n)$ becomes constructive for $\mathrm{Re} f_{K^+p}(s,0)$ and $\mathrm{Re} f_{K^+n}(s,0)$ due to the relative sign change between Eqs. (39) and (40). The same behavior can also be observed in the NN and $\bar{N}N$ amplitudes by comparison of the entries of Tables I and II. Thus the relative sizes of the predicted values of the $\rho_{\bar{K}N}$, ρ_{KN}, ρ_{NN}, and $\rho_{\bar{N}N}$ are easily understood in terms of the total cross sections.

Finally the forward differential cross sections for charge-exchange processes can also be predicted from the parameters of the total-cross-section analysis. In Fig. 9 the predicted values of $(d\sigma/dt)(s,0)$ for $\pi^- p \rightarrow \pi^0 n$ are compared with experimental measurements[23] at small momentum transfer for several energies. The experimental differential charge-exchange cross section increases from $t=0$ to $t\approx -0.1$ (BeV/c)^2 then turns over and decreases at larger t.[23,24] The predicted point is smaller than would be expected by simple extrapolation of the experimental points to $t=0$. The rapid increase of $d\sigma/dt$ at small t is presumably due to the helicity flip amplitude which vanishes at $t=0$. The value of $\alpha_\rho \approx \frac{1}{2}$ obtained in Eq. (22) gives equal real and imaginary parts for the $\pi^- p \rightarrow \pi^0 n$ amplitude. For the K^+n and K^-p charge-exchange reactions we qualitatively reproduce earlier predictions[2] that the $K^+n \rightarrow K^0 p$ amplitude is predominantly real[25] and the $K^-p \rightarrow \bar{K}^0 n$ amplitude is predominantly imaginary.

VI. DISCUSSION

The intent of this paper was the construction of a phenomenological peripheral model for the forward elastic-scattering amplitudes based on Regge poles with residues related by $SU(3)$ symmetry. We have tactily assumed that symmetry-breaking effects for the residues are relatively unimportant provided that comparisons are limited to quantities involving only the exchanges of the members of a single $SU(3)$ multiplet. For instance, since the Δ_{AB} depend only on the exchange of the vector meson nonet, we used $SU(3)$ related residues. Our justification for adopting such a procedure is based on a previous paper[12] in which the ρ-meson contribution to the Δ_{MB} was isolated. There the ratio of the ρ-meson couplings to the $\pi\pi$ and $\bar{K}K$ currents agreed to 15% with the exact $SU(3)$ value. However, when we must deal with quantities which depend on the exchanges of members of two $SU(3)$ multiplets X and Y, then the approximation of exact $SU(3)$ residues for each of the multiplets may not be adequate. In particular, if the exchange of multiplet X makes a much larger contribution than the exchange of multiplet Y, then failure to account for symmetry breaking in the residues of X may mask the actual contribution of Y. For example, the Σ_{AB} depend on exchanges of both the unitary singlet Pomeranchuk (P) and the members of the tensor nonet (T). Consequently we have not demanded $SU(3)$ symmetric residues for the large Pomeranchuk amplitude although we employed exact symmetry for the tensor nonet residues. The necessity of permitting symmetry breaking for the $P\pi\pi$ and $P\bar{K}K$ residues has been illustrated in Table I.

A unitary singlet meson (P) of maximal strength $\alpha_P=1$ and a nonet of tensor mesons (T) appears to be the most economic number of even C exchanges for explanation of the Σ_{AB}. Since the quantities Σ_{π^+p} and $\frac{1}{2}[\Sigma_{K^+p}+\Sigma_{K^+n}]$ show considerable variation with energy [cf. Fig. 6(a)] the existence of at least one $I=0$ secondary trajectory ($\alpha<1$) is implied. This observation eliminates from further consideration a proposed model which assumes no unitary singlet (P) but a tensor nonet (T) with $\alpha_{P'}\approx\alpha_S\approx 1$. Furthermore, a single $I=0$ secondary trajectory is insufficient either as a unitary singlet or as the $I=0$ member of an octet on the grounds that a unitary singlet would cause Σ_{π^+p} and $\frac{1}{2}[\Sigma_{K^+p}+\Sigma_{K^+n}]$ to fall at the same rate with energy where an $I=0$ octet member[2] would not reproduce the monotonic decreasing property of both Σ_{π^+p} and $\frac{1}{2}[\Sigma_{K^+n}+\Sigma_{K^+p}]$. Hence at least two $I=0$ secondary trajectories are required by the data. Since by the same reasoning both octet and singlet components must be invoked to explain the data, it is natural to associate the two $I=0$ secondary trajectories with the $I=0$ members of the 2^+ nonet.[7,26]

Since the meson-exchange model considered in this paper is consistent with all the high-energy total-cross-section data, the model is not only a means of understanding high-energy phenomena but also of determining parameters which are interesting in other contexts. In particular, for the zero-momentum-transfer

[23] I. Mannelli *et al.*, Phys. Rev. Letters **14**, 408 (1965).
[24] A. V. Stirling *et al.*, Phys. Rev. Letters **14**, 763 (1965).
[25] S. Goldhaber *et al.*, Phys. Rev. Letters **15**, 737 (1965).
[26] B. Desai and P. Freund, Phys. Rev. Letters **16**, 622 (1966).

couplings, we found that

(i) $(f/d)_{V\bar{B}B} \simeq (F/D)_{T\bar{B}B} \simeq -2$.
(ii) The $\langle T\rangle\langle\bar{B}B\rangle$ coupling strength must necessarily be large.

Finally, we might emphasize that more precise measurements of the total cross sections will permit considerable refinement of the present analysis (especially for the Σ_{AB}) and will check the validity of this approach to high-energy scattering.

ACKNOWLEDGMENTS

We thank Professor D. Cline and Professor C. Goebel for their interest in this work.

PHYSICAL REVIEW VOLUME 146, NUMBER 4 24 JUNE 1966

Application of an Approximate Solution of Partial-Wave Dispersion Relations to Yukawa Potential Scattering

J. REINFELDS
George C. Marshall Space Flight Center, Huntsville, Alabama

AND

J. SMITH*
Niels Bohr Institute, University of Copenhagen, Copenhagen, Denmark

(Received 12 January 1966)

The time-reversal symmetrization of the multichannel scattering amplitude proposed by Fulton and Shaw is used to construct the amplitude for nonrelativistic single-channel Yukawa potential scattering. It provides a modified determinantal method for the solution of the N/D equations. This amplitude is compared to the exact solution of the Schrödinger equation. It is found that the scattering lengths predicted by this method are qualitatively the same as those predicted by the full N/D equations and significantly better than the results of the determinantal method. The computational simplicity of the determinantal method has been retained and combined with the accuracy of the full N/D solution, which, with first-order Born approximation, gives quite a reliable picture of the qualitative features of the scattering.

I. INTRODUCTION

THE N/D method of finding the relativistic scattering amplitude for single-channel scattering entails the solution of an integral equation and the evaluation of an integral. One frequently uses the determinantal method, which reduces the problem to the evaluation of a single integral. Although simple to use, this method gives results which often differ significantly from the results predicted by the full N/D method. It was shown by Luming[1] that for nonrelativistic Yukawa potential scattering the exact Schrödinger solution lies close to the full N/D solution with both first and second Born approximation as input to the N/D equations. The determinantal solution, again using Born approximation for input, is quite unreliable in predicting the features of the scattering.

The ordinary determinantal method has no time-reversal symmetry when applied to the multichannel problem. A modification of the N/D equations was proposed by Fulton[2] and Shaw[3] to restore the time-reversal symmetry and the main purpose of this paper is to examine how this modification affects the single channel nonrelativistic scattering for which the exact solution can be found for comparison. Another such modification, proposed by Nath and Srivastava,[4] was examined by Smith.[5]

It is found that in the first-order Born approximation both of these methods give results in qualitative agreement with those of the N/D equations for all the angular-momentum states and coupling strengths examined, so that a considerable amount of computational labor can be saved by using a modified determinantal method. Calculations are in progress at present to include second-order Born terms in both methods and preliminary results show that one can obtain fairly good quantitative agreement between them.

The application of the N/D and determinantal method to Yukawa scattering was examined by Luming,[1] and the reader is referred to that paper for details. A short discussion of the Fulton-Shaw method is given in Sec. II. The application to potential theory is discussed in Sec. III, where the effective-range expressions are derived. Finally, in Sec. IV, we give the results of the calculations, which were performed on the AMTRAN self-programming computer system, and our conclusions.

* Present address: Department of Mathematical Physics, University of Adelaide, South Australia.
[1] M. Luming, Phys. Rev. **136**, B1120 (1964).
[2] T. Fulton, in *Brandeis Lecture Notes, 1962* (W. A. Benjamin and Company, Inc., New York, 1963), Vol. I, p. 55.
[3] G. Shaw, Phys. Rev. Letters **12**, 345 (1964).
[4] P. Nath and Y. K. Srivastava, Phys. Rev. **138**, B1195 (1965).
[5] J. Smith (to be published).